Conditioning films formed by algal biopolymers in seawater reverse osmosis desalination

David A. Ladner[1,2], John A. Jurevis[1], Mark M. Clark[1,3]

[1]University of Illinois at Urbana-Champaign, Civil and Environmental Engineering [2]Arizona State University, School of Sustainable Engineering and the Built Environment [3]Northwestern University, Civil and Environmental Engineering

Overview

Fouling of reverse osmosis membranes in desalination facilities is heavily exacerbated by marine algal blooms (like "Red Tides"). The algae themselves are not the fouling culprits because they are large enough (roughly 10 to 50 µm) to be removed by pretreatment systems. Biopolymers released from the algal cells, however, can pass through pretreatment and adsorb to the reverse osmosis (RO) membranes. These biopolymers form a conditioning film that changes the surface properties of the membranes and can enhance biofilm development. This project seeks to characterize algal biopolymers and their interactions with RO membranes.

Materials and Methods

Heterocapsa pygmaea algae were cultured in the laboratory (Fig. 1). Bench-scale RO experiments were performed with commercial membranes (Fig. 2). Analytical tools included visual imaging, laser scanning cytometry (LSC), scanning electron microscopy (SEM), attenuated total reflectance Fourier transform infrared spectroscopy (ATR-FTIR), wet-chemical protein and carbohydrate determination, and polyacrylamide gel electrophoresis (SDS-PAGE).

Results and Discussion

When algae were spiked directly to the RO system some flux decline occurred; however, little if any change in performance was seen when the particles were removed and only organic matter remained (Fig. 3). Visual imaging could not easily detect the organic matter, though fluorescence imaging using LSC gave some detection (Fig. 4). With SEM it is clear that not much organic matter accumulated when particles were removed, but a patchy conditioning film did begin to accumulate. The patchiness suggests the organic matter (biopolymers) prefer to stick to each other rather than the membrane. Infrared absorbance gave some indication of proteins (1540 and 1640 cm^{-1}) and carbohydrates (3230 and 900-1080 cm^{-1}) present in the conditioning film (Fig.6). Wet-chemical analysis showed proteins were more abundant than carbohydrates in the film (Fig. 7), even though carbohydrates were more abundant in the feed water (Fig. 8). Some of the proteins were contained within larger cellular pieces and could be filtered out on 0.45 and 0.22 µm membranes, but a significant fraction were dissolved and only removable by tighter ultrafilters (Fig. 9). Breakup of the cell with shear released proteins into the water matrix. At least seven different algal proteins were present and adsorbed to the RO membranes (Fig. 10). Experiments to determine which proteins adsorbed most readily have proven inconclusive; all proteins present seem to stick to the RO membranes.

Conclusions

Algal biopolyers do not show a very strong affinity for RO membranes, nor do they decrease RO water flux in and of themselves. But they do accumulate and form a conditioning film. Proteins are more prominent in this film than carbohydrates. Work continues to determine which proteins have the greatest adsorption affinity.

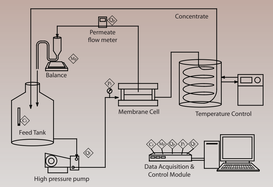

Figure 2. Diagram of the bench-scale SWRO membrane testing unit. Diamond symbols indicate electronic interface between the computer and components. Automated data acquisition locations are shown for feed conductivity (Cf), feed pressure (Pf), permeate flow rate (Qp), and permeate mass (Mp). Automated control of the high-pressure pump, and thereby the feed flow rate (Qf), is also indicated.

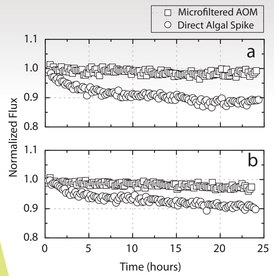

Figure 3. Normalized RO specific flux for microfiltered algogenic organic matter (AOM) and direct algal spikes (40,000 cells/ml) on (a) SW30HR membranes and (b) SWC4 membranes.

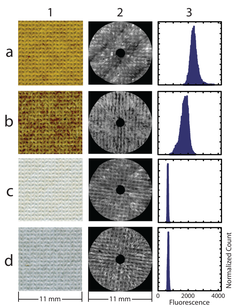

Figure 4. (Column 1) Visual images, (Column 2) LSC fluorescence images, and (Column 3) fluorescence histograms of RO membranes fouled by algogenic organic matter. (a) Direct algal spike, SW30HR; (b) Direct algal spike, SWC4; (c) Microfiltered AOM, SW30HR; (d) Microfiltered AOM, SWC4. In LSC images (2) contrast was adjusted to highlight notable features so grey levels are not comparable among images. Histogram heights in (3) were normalized to the maximum peak heights.

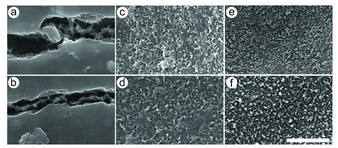

Figure 5. SEM images of fouled and clean RO membranes. (a) Direct algal spike, SW30HR. (b) Direct algal spike, SWC4. (c) Microfiltered AOM, SW30HR. (d) Microfiltered AOM, SWC4. (e) Clean SW30HR. (f) Clean SWC4. Images were taken at 20 kV in secondary electron imaging mode with 20 kV acceleration voltage. White scale bar spans five µm.

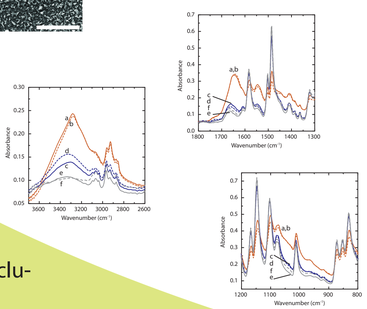

Figure 6. Infrared absorbance spectra of fouled and clean RO membranes in the wavenumber regions 3700 to 2600 cm-1, 1800 to 1300 cm-1, and 1200 to 800 cm-1. (a) Direct algal spike, SW30HR. (b) Direct algal spike, SWC4. (c) Microfiltered AOM, SW30HR. (d) Microfiltered AOM, SWC4. (e) Clean SW30HR. (f) Clean SWC4.

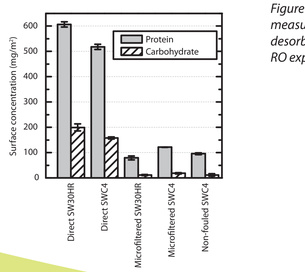

Figure 7. Surface protein and carbohydrate concentrations of fouled RO membranes after direct spikes of algae and microfiltered AOM. Error bars span standard error of triplicate measurements.

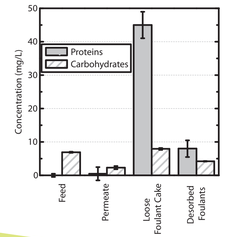

Figure 8. Protein and carbohydrate concentrations measured for feed, permeate, loose foulant cake, and desorbed foulants in an algal-fouling bench-scale RO experiment.

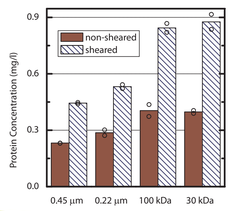

Figure 9. Protein concentrations extrapolated from direct measurement of membranes of different pore sizes used to filter sheared and non-sheared algal samples. The concentration shown is the amount of protein in the feed water that was collectable by that membrane. Circles give actual measurements (2 repetitions per sample) and bars show averages.

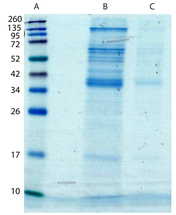

Figure 10. Stained SDS-PAGE gel showing (A) the molecular weight marker with protein sizes [kDa] labeled, (B) proteins released from algae by physical breakup, and (C) a protein sample exposed to an RO membrane.

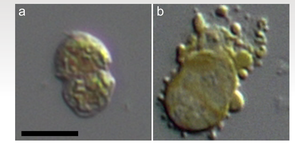

Figure 1. (Main area) Structural features of H. pygmaea algae. (a) Thecal plates and their designations; ': apicals, ": precingulars, "": postsingulars, "": antapicals, as: anterior sulcal, rs: right sulcal, las: left anterior sulcal, lps: left posterior sulcal, ps: posterior sulcal. Plate locations and designations are from Loeblich et al. (1981). (b) Cross-sectional view of internal organelles as seen in TEM images (Bullman and Roberts 1986). (c) Typical morphology and orientation of flagella as seen in SEM images (Roberts et al. 1987). Scale bar is five microns. (Top right) H. pygmaea was grown in the laboratory in these glass containers illuminated with fluorescent bulbs. (Middle right). (a) Visible-light microscope image of an H. pygmaea algal cell. (b) A cell that was crushed under the microscope slide to demonstrate release of algal biopolymers. In seawater desalination plants such a release could be caused by shear in intake structures, pumps, and valves.

David A. Ladner
david.ladner@asu.edu
217-493-8150
http://davidladner.org

Primary Funding: Water Research Foundation, project 04201
Other funding from the U.S. Environmental Protection Agency (STAR fellowship program) and the US Bureau of Reclamation assistance agreement 05FC811169

ILLINOIS
UNIVERSITY OF ILLINOIS AT URBANA-CHAMPAIGN

Ira A. Fulton Schools of Engineering
ARIZONA STATE UNIVERSITY